Electrically Driven Reversible Insulator−Metal Phase Transition in 1T-TaS₂

Matthew J. Hollander,*,† Yu Liu,‖ Wen-Jian Lu,‖ Li-Jun Li,‖ Yu-Ping Sun,*,‖,⊥,# Joshua A. Robinson,‡,§ and Suman Datta*,†

†Electrical Engineering Department, ‡Materials Science and Engineering Department, and §Center for 2-Dimensional and Layered Materials, The Pennsylvania State University, University Park, Pennsylvania 16802, United States

‖Key Laboratory of Materials Physics, Institute of Solid State Physics, and ⊥High Magnetic Field Laboratory, Chinese Academy of Sciences, Hefei 230031, People's Republic of China

#Collaborative Innovation Centre of Advanced Microstructures, Nanjing University, Nanjing 210093, People's Republic of China

S Supporting Information

ABSTRACT: In this work, we demonstrate abrupt, reversible switching of resistance in 1T-TaS₂ using dc and pulsed sources, corresponding to an insulator−metal transition between the insulating Mott and equilibrium metallic states. This transition occurs at a constant critical resistivity of 7 mohm-cm regardless of temperature or bias conditions and the transition time is significantly smaller than abrupt transitions by avalanche breakdown in other small gap Mott insulating materials. Furthermore, this critical resistivity corresponds to a carrier density of 4.5×10^{19} cm^{-3}, which compares well with the critical carrier density for the commensurate to nearly commensurate charge density wave transition. These results suggest that the transition is facilitated by a carrier driven collapse of the Mott gap in 1T-TaS₂, which results in fast (3 ns) switching.

KEYWORDS: Mott insulator, resistive switching, insulator−metal-transition, charge density wave, 1T-TaS₂
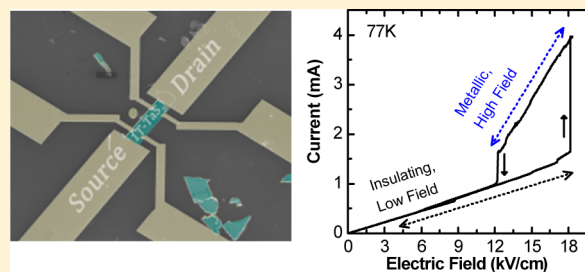
The transition metal dichalcogenide 1T-TaS₂ is a two-dimensional (2D) layered material exhibiting interesting and complex behavior as a result of interplay between electron−electron and electron−lattice interactions. Below 600 K, 1T-TaS₂ is host to several distinct charge density wave (CDW) phases, which exist as a result of Fermi-surface driven instabilities (i.e., Fermi-surface nesting) that lead to a distortion of the crystal lattice and subsequent periodic charge density modulation. These charge and structural distortions eventually become fully commensurate with the lattice below a critical temperature of ∼180 K, after which electron−electron interactions lead to the formation of an insulating state through a Mott−Hubbard transition.[1,2] Recent work has explored ultrafast melting of the insulating Peierls−Mott state using pulsed optical or electronic means in order to partially collapse the Mott gap or to produce metastable states of intermediate resistivity and variable duration.[3−6] In this work, we demonstrate abrupt, resistive switching between insulating and conducting states through electronic means. Both dc and pulsed voltages are used to trigger abrupt resistive switching from the insulating Mott phase to the metallic phase. After the applied electric field is removed, the 1T-TaS₂ undergoes a second abrupt transition and returns to its equilibrium insulating state. In this fashion, the material functions as an abrupt electrically driven volatile switch. Importantly, this transition is shown to occur at a resistivity of 7 mohm-cm

regardless of temperature or bias conditions and the transition time of 3 ns is significantly smaller than abrupt transitions by avalanche breakdown in other small gap Mott insulating materials. Furthermore, this critical resisitivity corresponds to a carrier density of 4.5×10^{19} cm^{-3}, which compares well with the critical carrier density for the commensurate to nearly commensurate charge density wave transition. These results suggest that the observed transition may be caused or facilitated by a carrier driven collapse of the Mott gap, which results in a fast (3 ns) collapse of the insulating state.

Figure 1a shows the atomic structure of 1T-TaS₂ as well as the characteristic "Star-of-David" distortion of the Ta lattice. This distinctive distortion is the result of Fermi-surface nesting and is accompanied by out-of-plane distortions of the coordinating S atoms such that the sulfur lattice bulges slightly around the center of the "star."[2,7,8] As the temperature is varied from 600−0 K, three distinct phases of 1T-TaS₂ are observed. Figure 1d plots resistivity versus temperature of a 10 nm thick 1T-TaS₂ flake and captures these three equilibrium phases. The low-temperature insulating phase is structurally the most simple of the three. This phase is referred to as the commensurate CDW (CCDW) phase because in this phase, the "Star-of-
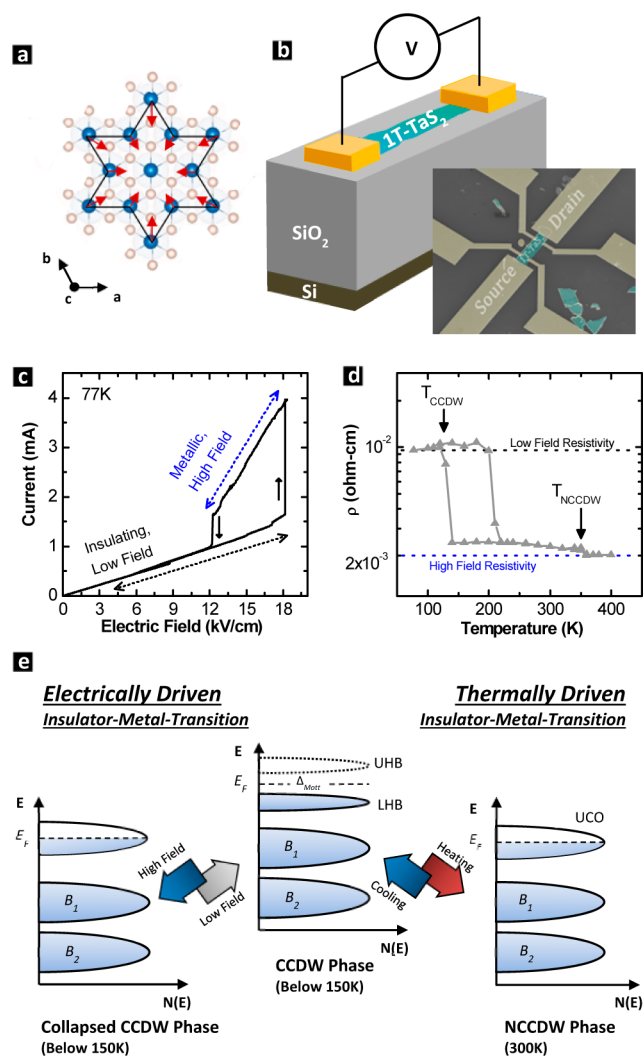
Figure 1. Schematic representation of 1T-TaS$_2$ structure (a) and two terminal device (b). Inset shows colorized SEM micrograph of Hall bar structure (b). Typical current−voltage sweep showing abrupt transition to metallic phase and return to insulating phase (c). Low- and high-field resistivities extracted from current−voltage sweep at 77 K superimposed on resistivity versus temperature (d). Energy diagram showing electrically and thermally driven collapse of the Mott gap (e).

David" distortions interlock to form a triangular superlattice that is fully commensurate with the crystal lattice. In the CCDW phase, the 12 surrounding Ta atoms contract toward the 13th central Ta atom and become strongly bonded to each other. This results in two low-lying three-band submanifolds (B_1 and B_2 in Figure 1e) representing the 12 outer atoms and one narrow band at the Fermi energy, E_F, corresponding to the central Ta atom.[9] Because of the small width of this band (∼100 meV) and its half-filled nature, it has been proposed that Mott localization occurs as a result of electron−electron interactions.[2] The opening of a Mott gap (200 meV) leads to a sharp jump in resistivity and insulating behavior below ∼180 K. Above this temperature, the "Star-of-David" distortions remain, but no longer form the interlocking triangular superlattice that is commensurate with the lattice. Instead, they form roughly hexagonal domains that are separated by small triangular regions that are incommensurate with the lattice.[8] Here, the hexagonal domains remain commensurate with the lattice. This phase is referred to as the nearly commensurate CDW

(NCCDW) phase and does not exhibit the insulating behavior of the CCDW phase. The NCCDW phase exhibits a resistivity range of approximately 5−0.5 mohm-cm, roughly 10× reduced from the CCDW phase. This resistivity range is a common feature of the 1T-TaS$_x$Se$_{1−x}$ material family and is of importance in the sense that it is centered about 3 mohm-cm, which is the resistivity value if one were to assume the universal value of the maximum metallic resistivity for each 2D layer of the crystal.[2] Above 350 K, the distortions become even more incommensurate with the underlying lattice and 1T-TaS$_2$ undergoes a 2× drop in resistivity; this is referred to as the incommensurate CDW phase (ICCDW).

Although previous works have investigated interplay between these phases by examining the collapse of the insulating Mott phase using time-resolved, angle-resolved photoelectron spectroscopy in an ultrafast pump−probe configuration, these studies focused primarily on understanding the mechanisms that govern charge and lattice reordering under nonequilibrium conditions and under the influence of electric field.[3,4] Alternatively, Stojchevska et al. have recently presented work showing the presence of hidden metastable states below 50 K that are reached after a short excitation pulse (∼30 fs) is applied to the CCDW phase. It is thought that these states are a result of voids due to hole recombination with the conduction electron isolated on the central Ta atom.[5] These voids are distributed across the sample and contribute to conductivity through formation of incommensurate regions.[5] The authors postulate that if they can be stabilized with some kind of long-range order before they can annihilate, then the material can be locked in a quasi-stable low resistivity state. After entering the hidden state, the 1T-TaS$_2$ remains there until an erase pulse is applied to the sample for a long enough time to allow thermalization of the electron−hole variations or by heating the sample. Most recently, Vaskivskyi et al. have probed these hidden metastable states using electrical means. In their work, these states are reached after applying a short voltage pulse in order to asymmetrically introduce charge to the CCDW system.[6] The original CCDW state cannot be recovered by increasing the applied voltage pulse magnitude or duration. Instead, application of a longer duration pulse only partially recovers the insulating behavior of the CCDW. As in previous work, these hidden states can be completely erased by heating the sample.

In this work, two-terminal dc and pulsed voltages and currents are used to demonstrate abrupt, resistive switching between the various phases of 1T-TaS$_2$ over a range of temperatures (77−150 K). Figure 1b shows a schematic representation of a two-terminal device along with a colorized scanning electron microscopy (SEM) micrograph. 1T-TaS$_2$ flakes on SiO$_2$ substrates (190 nm) are prepared from bulk 1T-TaS$_2$ crystals using an exfoliation process. The 1T-TaS$_2$ single crystals are grown using a chemical vapor transport method to produce a TaS$_2$ powder, that was subsequently heated in a sealed quartz tube and quenched to retain the 1T phase. Additional details are provided in the Supporting Information. Flakes are identified optically and metal contacts are patterned using electron beam photolithography (Ti/Au, 10/50 nm). A post metallization forming gas anneal at 450 °C is used to ensure that the metal leads make good contact to the 1T-TaS$_2$. Flake thickness is measured by atomic force microscopy, with flakes ranging in thickness from 8−55 nm (14−95 atomic layers). A representative current−voltage (I−V) measurement is plotted in Figure 1c showing an abrupt

reduction in resistivity after reaching a critical field. This measurement is performed at 77 K in high vacuum for a 1T-TaS$_2$ flake with length 8.4 μm, width 6.6 μm, and thickness 10 nm (17 layers). Figure 1d plots the resistivity versus temperature of the same flake, which is extracted from two-terminal measurements.

For this voltage-mode measurement (*V*-mode, Figure 1c), the voltage across the device is swept from 0 to 20 V and back to 0 V while measuring the current through the device. In the low field regime, the flake exhibits a linear *I*−*V* response with a resistivity of approximately 9 mohm-cm. We find that the resistivity of the flake in this regime remains constant over a broad range and matches closely with the resistivity of the CCDW phase (which is the equilibrium phase at this temperature). Figure 1d superimposes the extracted low-field resistivity from the 2-terminal *I*−*V* characteristics (black dashed line) on the resistivity versus temperature plot. After reaching a critical threshold electric field and threshold current (18 kV/cm, 1.5 mA), the current through the flake increases abruptly. After this abrupt transition, the *I*−*V* response remains linear in nature, but indicates a resistivity roughly 10× lower than the initial insulating CCDW phase. This reduced resistivity (blue dashed line) matches with the resistivity of the NCCDW or ICCDW phases (Figure 1d), suggesting that the flake has undergone an abrupt transition from the insulating to metallic phase. On the return sweep back to zero bias, the flake undergoes another abrupt transition after reaching another critical point (12 kV/cm, 1 mA). In this transition, the flake switches from the metallic state back to its original insulating state.

The abrupt and reversible change in resistivity observed in this work may be a result of one of several mechanisms. An insulator-to-metal transition (IMT) can occur in conventional insulating materials by mechanisms such as avalanche or Zener breakdown where application of large electrical field leads to impact ionization or direct tunneling of the carrier across the band gap, respectively. For Mott insulators, an IMT can occur through an additional mechanism: the collapse of the Mott gap. This can be realized by surpassing a critical carrier concentration such that the electron−electron interactions that lead to Mott−Hubbard localization can be screened out. The critical carrier concentration at which the Mott gap collapses is defined according to the Mott criterion: $n_c^{1/3} a_H \approx 0.25$.[10] Here, a_H is the effective Bohr radius and n_c is the critical carrier density to initiate the insulator-to-metal transition from the insulating state. The effective Bohr radius can be calculated according to $a_H = (\varepsilon h^2/4\pi^2 m^* e^2)$, where ε is the permittivity of the material and m^* represents the effective mass of the charge carrier. Alternatively, n_c can be approximated by determining n_s, the equilibrium carrier density in the insulating state as the insulator-to-metal transition threshold is approached. In other Mott insulators, the value of n_c has been found to be of the order of n_s.[11]

In the case of bulk 1T-TaS$_2$, Hall effect measurements can be utilized to determine n_s and, subsequently, n_c. Hall effect measurements on bulk 1T-TaS$_2$ used in this work indicate a carrier density of approximately 2.5 × 10^{19} cm^{-3} and a carrier mobility of approximately 20−15 cm^2/V·sec at a temperature of 150 K. Inada et al. show a monotonic increase in carrier density from roughly 5 × 10^{18} to 5 × 10^{19} cm^{-3} as temperature is increased from 50 to 200 K,.[12] Within this temperature range, the Hall effect data is consistent with a single carrier model and the carriers are found to be hole like (p-type). As the

temperature is increased further toward the CCDW to NCCDW transition point, the carrier concentration within the 1T-TaS$_2$ saturates at a value of approximately 5 × 10^{19} cm^{-3}. At the transition point, it exhibits a sudden increase in carrier density to approximately 5 × 10^{21} cm^{-3}, which subsequently increases with increasing temperature to values as high as 2 × 10^{22} cm^{-3} at temperatures above 350 K (i.e., the ICCDW phase).[12] These data compare well with the measured carrier density and mobility in this work, indicating an n_s of ∼5 × 10^{19} cm^{-3}.

Abrupt changes in resistivity can be realized through additional mechanisms as well. In the case of CDW materials, sliding CDW conduction is one such mechanism, where CDWs that are initially pinned at a defect site can be triggered by application of an external field.[13,14] Although sliding CDW conduction leads to an abrupt increase in conduction through the material, it typically does not lead to a sharp jump to higher currents, but instead exhibits a kink or elbow in the *I*−*V* relationship.[15−17] Furthermore, the critical fields at which CDW sliding occurs are typically below 1 kV/cm, which is over an order of magnitude lower than the critical field observed in this work.[16] Additionally, Hall et al. utilized a temperature-dependent investigation into CDW depinning in NbSe$_3$ in order to distinguish between "CDW sliding" and "CDW switching". CDW sliding was shown to result in a kink type transition in the *I*−*V* response while CDW switching was shown to result in an abrupt change in resistivity.[17] Although they were unable to pinpoint the exact mechanism by which CDW switching occurred, Hall et al. were able to show that these were two distinct phenomenon, which can be triggered separately at two distinct critical fields.[17] IMTs may also occur without field assistance (i.e., avalanche and Zener breakdown) or carrier assistance (i.e., satisfying the Mott criterion). Many IMTs are thermally driven, such as the case for perovskite rare-earth nickelates, or may be driven by local Joule heating as current flows through the material.

Figure 2a plots the critical fields for avalanche and Zener breakdown as a function of bandgap and the typical range of critical fields observed in this work for the IMT in 1T-TaS$_2$ (marked with red line). Although dielectric breakdown in Mott insulators has been investigated theoretically in various studies, few experimental reports exist detailing the phenomenon. Recently, Guiot et al. studied resistive switching of several small gap Mott insulators in the GaTa$_4$Se$_{8-x}$Te$_x$ family induced by electronic breakdown of the Mott insulating state.[18] In their work, a dependency on the critical threshold field for the IMT was found according to the universal law of $E_{th} \propto E_{gap}^{2.5}$ for avalanche breakdown. According to their results, this dependency predicts a critical threshold field of roughly 3 kV/cm for 1T-TaS$_2$ in the Mott insulating state (E_g = 200 meV). In this work, the observed threshold fields for 1T-TaS$_2$ range from 10 to 20 kV/cm. Although the observed E_{th} is substantially larger than that predicted for avalanche breakdown, they are significantly lower than that predicted for Zener breakdown by tunneling across the Mott gap.[19]

In order to probe the field, temperature, and carrier dependency of the IMT in 1T-TaS$_2$, voltage and current mode measurements were performed as a function of temperature. Figure 2b plots *V*-mode measurements as a function of temperature from 77 to 150 K. Above ∼150 K, 1T-TaS$_2$ exists in the metallic NCCDW phase as its equilibrium state. Again, the voltage across the device is swept from 0−20 V and back to 0 V while measuring the current through the
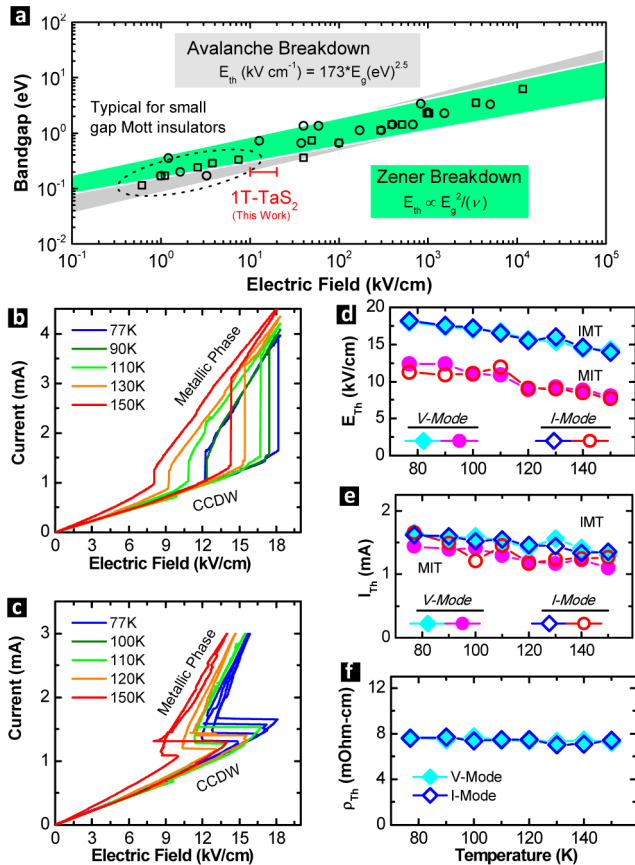
Figure 2. Plot of critical fields for avalanche and Zener breakdown mechanisms as a function of bandgap (a). Voltage-mode measurements (b) and current-mode measurements (c) of 1T-TaS$_2$ as a function of temperature. Critical electric field (d), current (e), and resistivity (f) at the IMT point as a function of temperature for voltage and current-mode measurements.

device. Current mode (*I*-mode) measurements are also performed (Figure 2c), wherein the current sourced through the flake is swept from 0−3 mA and back to 0. For both measurement techniques, an abrupt transition from CCDW to metallic phase is observed. The absolute field and current at the IMT and metal-to-insulator transition (MIT) points are plotted as a function of temperature for the *V*- and *I*-mode measurements in Figure 2d,e. The threshold field (E_{th}) and threshold current (I_{th}) appear to be independent of measurement mode. Both *V*- and *I*-mode measurements show E_{th} and I_{th} that monotonically decrease with increasing temperature. Although the low-field (low-current) I−V response exhibits linear behavior, we note that as the transition point is approached the I−V response begins to show a superlinear behavior while others have reported exponential behavior.[6] Exponential dependency of current density on voltage may be indicative of an increase in carrier density due to impact ionization, which can be thought of as a doping process, which introduces additional carriers to the system.[20] Another possible source for the superlinear behavior is the conduction due to sliding CDWs after reaching a critical depinning threshold field.

Extracting the resistivity at the transition point, we find a constant critical resistivity, ρ_c, of 7 mohm-cm that is independent of both temperature and measurement mode. Similar behavior for a metal-to-insulator transition has also been reported for the case of VO$_2$, where it has been suggested

that a critical threshold resistivity is indicative of a critical carrier density that triggers the phase transition.[21] Considering the measured ρ_c and assuming a carrier mobility of 20 cm^2/V·sec, the critical resistivity of 7 mohm-cm corresponds to a critical carrier density, n_c, of ~4.5 × 10^{19} cm^{-3}, which compares well with the measured n_s at the insulator-to-metal transition in 1T-TaS$_2$.[17] This mobility was selected based on experimental results in the literature.[17] Furthermore, this critical carrier density can be used to calculate an effective Bohr radius according to the Mott criterion. Using the n_c calculated from the constant critical resistivity, an effective Bohr radius of 6.9 Å is found.

In order to probe the IMT further, a V-mode measurement was performed with varying resistances in series with the 1T-TaS$_2$ flake. Figure 3a shows a schematic representation of the
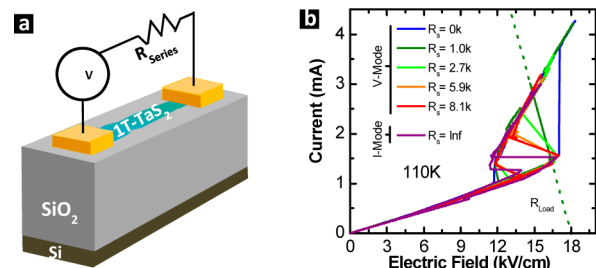
Figure 3. Schematic representation of measurement setup (a). Current−voltage characteristics as a function of series resistor (b) showing abrupt switching and negative differential resistance for the insulator−metal and metal−insulator transitions.

measurement setup while Figure 3b plots the measured results for different series resistances at 110 K. Here, the current through the device is calculated by considering the bias conditions and series resistor. An *I*-mode measurement is plotted for comparison. Viewing the ideal current source as an open circuit, one may consider the *I*-mode measurement equivalent to a *V*-mode measurement with series resistance that is effectively infinite. Use of a resistor in series with the flake produces a negative differential resistance across the IMT as well as the MIT, where the slope of the negative differential resistance can be related to the series resistance (R_{Load}, Figure 3b). Here, the "s"-shaped character of the I−V sweep and the negative differential resistance point to a carrier (current) driven process. Negative differential resistance is also observed for avalanche breakdown, which can be viewed as, effectively, a carrier driven process.[18]

The time scale of the IMT was investigated using pulsed *V*-mode measurements. In order to capture the voltage across the 1T-TaS$_2$ flake while pulsing, a load resistor (R_s) was placed in series with a flake and the output waveform was captured as the voltage measured across R_s. In this experiment, the flake used was 4 μm long, 13 μm wide, and roughly 20 nm thick. All pulse measurements were made at a temperature of 150 K. Figure 4a shows a schematic representation of the setup while Figure 4b shows the input voltage waveform. A triangular pulse was used so that the IMT could be captured in the output waveform and the critical fields, currents, and resistivities could be extracted for each pulsed measurement. The pulse width was varied from 3 s to 30 μs. Figure 4c shows a pair of representative input and output waveforms (t_{pulse} = 300 μs). Within the measured output waveform, an abrupt transition from lower voltage to higher voltage is observed. This behavior indicates an IMT within the
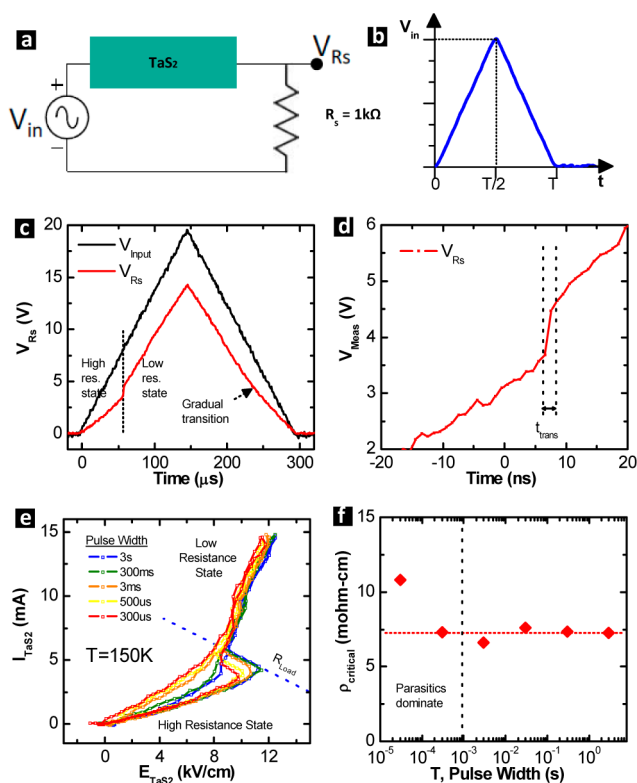
Figure 4. Schematic representation of pulsed $I-V$ measurement setup (a) and representative input waveform (b). Input and measured voltage across R_s for a 300 μs pulse (c). Zoomed-in view of abrupt, sub-10 ns IMT (d). Reconstructed pulsed $I-V$ curves as a function of pulse width showing negative differential resistance (e). Extracted critical resistivity as a function of pulse width (f).

1T-TaS$_2$, where an abrupt reduction in TaS$_2$ resistance leads to a sharp increase in voltage dropped across R_s. The time duration of the IMT is found to be less than the time resolution of the oscilloscope (<10 ns) (Figure 4d). Higher-resolution oscilloscope captures show a $t_{trans} \sim 3$ ns, which is significantly smaller than other narrow gap Mott insulators (10 μs to 1 ms).[18] Such short transition times, as well as the significantly higher critical field observed in this work compared to avalanche breakdown in other small gap Mott insulators may indicate that the abrupt IMT in 1T-TaS$_2$ is not an avalanche breakdown process. On the other hand, previous work in 1T-TaS$_2$ has shown that collapse of the Mott gap and subsequent charge reordering can take place in the subpicosecond time scale, while reordering of the lattice follows within pico-seconds.[3,4]

By calculating the voltage across the 1T-TaS$_2$ flake as well as the current through the device, a pulsed $I-V$ plot can be constructed for each discrete pulse. Figure 4e plots the pulsed $I-V$ data for five different pulse widths. Here, we plot a smoothed and interpolated trace of the pulsed $I-V$ data as a result of significant noise introduced by subtraction of the two captured waveforms. Similar to the dc results, the pulsed $I-V$ shows an abrupt transition at a critical field (11 kV/cm). Although variation in the critical threshold field was found across these and other fabricated devices, no significant trend was found with source-drain spacing or geometric factors. The change in resistivity across the IMT is found to be roughly 10×, which is expected for a transition from CCDW to NCCDW. Additionally, the critical resistivity for the IMT is extracted

from the pulsed $I-V$ and plotted as a function of pulse width in Figure 4e. A value of $\sim$7.5 mohm-cm is extracted for pulse widths ranging from 3 s to 300 μs. . The critical resistivity extracted from the longer pulse widths matches with the dc data and further supports the idea that the abrupt switching behavior is the result of a carrier driven collapse of the Mott insulating state. For the pulsed $I-V$ with pulse width below 300 μs, RC time delay from parasitic capacitances in the cabling and measurement setup begin to dominate, which result in artificially high critical resistivities.

1T-TaS$_2$ represents an interesting material for study of correlated phases in low-dimensionality materials with several competing equilibrium states and a Mott insulating phase. Recent work has explored ultrafast melting of 1T-TaS$_2$'s insulating Mott state using pulsed optical or electronic means to produce metastable states of intermediate resistivity and variable duration. In this work, we have probed the abrupt, resistive switching between equilibrium states using dc and pulsed voltages as well as dc current sourcing. An abrupt reduction in resistivity corresponding to a phase transition from the Mott state to the metallic phase is observed for both V-mode and I-mode as well as pulsing down to a minimum pulse width of 30 μs Importantly, this phase transition is shown to occur at a constant critical resistivity of 7 mohm-cm regardless of temperature or bias conditions and the transition time is significantly smaller than abrupt transitions by avalanche breakdown in other small gap Mott insulating materials that occur in a time range of 10 μs to 1 ms. Furthermore, the measured critical resistivity is shown to correspond to a carrier density of 4.5×10^{19} cm^{-3}, which compares well with the observed critical carrier density for the CCDW to NCCDW transition. These results suggest that the transition is facilitated by a carrier driven collapse of the Mott gap in 1T-TaS$_2$ insulating state, which results in fast (3 ns) switching.

■ ASSOCIATED CONTENT

ⓢ Supporting Information

Synthesis and fabrication details. Additional resistivity versus temperature plots are included for flakes of varying thicknesses. This material is available free of charge via the Internet at http://pubs.acs.org.

■ AUTHOR INFORMATION

Corresponding Authors

*E-mail: (M.J.H.) mjh423@psu.edu.
*E-mail: (Y.-P.S.) ypsun@issp.ac.cn.
*E-mail: (S.D.) sdatta@engr.psu.edu.

Notes

The authors declare no competing financial interest.

■ ACKNOWLEDGMENTS

■ REFERENCES

(1) Fazekas, P.; Tosatti, E. Charge Carrier Localization in Pure and Doped 1T-TaS$_2$. *Physica B* **1980**, *99*, 183−187.

(2) Fazekas, P.; Tosatti, E. Electrical, structural and magnetic-properties of pure and doped 1T-TaS$_2$. *Philos. Mag. B* **1980**, *39*, 229−244.

(3) Sohrt, C.; Stange, A.; Bauer, M.; Rossnagel, K. How fast can a Peierls-Mott insulator be melted? *Faraday Discuss.* **2014**, *171*, 243−257.

(4) Perfetti, L.; Loukakos, P. A.; Lisowski, M.; Bovensiepen, U.; Wolf, M.; Berger, H.; Biermann, S.; Georges, A. Femtosecond dynamics of electronic states in the Mott insulator 1T-TaS$_2$ by time resolved photoelectron spectroscopy. *New J. Phys.* **2008**, *10*, 053019.

(5) Stojchevska, L.; Vaskivskyi, I.; Mertelj, T.; Kusar, P.; Svetin, D.; Brazovskii, S.; Mihailovic, D. Ultrafast switching to a stable hidden topologically protected quantum state in an electronic crystal. 2014, http://arxiv.org/abs/1401.6786 (accessed Sept 20, 2014).

(6) Vaskivskyi, I.; Mihailovic, I. A.; Brazovskii, S.; Gospodaric, J.; Mertelj, T.; Svetin, D.; Sutar, P.; Mihailovic, D. Fast non-thermal switching between macroscopic charge-ordered quantum states in duced by charge injection. 2014, http://xxx.tau.ac.il/abs/1409.3794 (accessed Sept 20, 2014).

(7) Wilson, J. A. Questions concerning the form taken by the charge-density wave and the accompanying periodic-structural distortions in 2H-TaSe$_2$, and closely related materials. *Phys. Rev. B* **1978**, *17*, 10.

(8) Spijkerman, A.; de Boer, J. L.; Meetsma, A.; Wiegers, G. A. X-ray crystal-structure refinement of the nearly commensurate phase of 1T-TaS$_2$ in (3 + 2)-dimensional superspace. *Phys. Rev. B* **1997**, *56*, 13757.

(9) Rossnagel, K.; Smith, N. V. Spin-orbit coupling in the band structure of reconstructed 1T-TaS$_2$. *Phys. Rev. B* **2006**, *73*, 073106.

(10) Mott, N. The transition to the metallic state. *Philos. Mag.*, **1961**, Vol. *6*, No. 62, 287−309.

(11) Ruzmetov, D.; Heiman, D.; Claflin, B. B.; Narayanamurti, V.; Ramanathan, S. Hall Carrier Density and Magnetoresistance Measurements in Thin-Film Vanadium Dioxide Across the Metal-Insulator Transition. *Phys. Rev. B* **2009**, *79*, 153107.

(12) Inada, R.; Onuki, Y.; Tanuma, S. Hall Effect of 1T-TaS$_2$. *Phys. Lett.* **1979**, *69A* (6), 453−456.

(13) Lee, P. A.; Rice, T. M. Electric field depinning of charge density waves. *Phys. Rev. B* **1979**, *19*, 8.

(14) Gruner, G.; Zawadowski, A.; Chaikin, P. M. Nonlinear Conductivity and Noise due to Charge-Density-Wave Depinning in NbSe$_3$. *Phys. Rev. Lett.* **1981**, *46*, 511.

(15) Adelman, T. L.; Zaitse-Zotov, S. V.; Thorne, R. E. Field-effect Modulation of Charge-Density-Wave Transport in NbSe$_3$ and TaS$_3$. *Phys. Rev. Lett.* **1995**, *74* (26), 5264−5267.

(16) Markovic, N.; Dohmen, M. A. H.; van der Zant, H. S. J. Tunable Charge-Density Wave Transport in a Current-Effect Transistor. *Phys. Rev. Lett.* **2000**, *84* (3), 534−537.

(17) Hall, R. P.; Zettl, A. Charge Density Wave Depinning and Switching in NbSe$_3$. *Solid State Commun.* **1984**, *50* (9), 813−816.

(18) Guiot, V.; Cario, L.; Janod, E.; Corraze, B.; Ta Phuoc, V.; Rozenberg, M.; Stoliar, P.; Cren, T.; Roditchev, D. Resistive switching induced by electronic avalanche breakdown in GaTa$_4$Se$_{8-x}$Te$_x$ narrow gap Mott Insulators. *Nat. Commun.* **2013**, *4*, 1722.

(19) Eckstein, M.; Oka, T.; Werner, P. Dielectric Breakdown of Mott Insulators in Dynamical Mean-Field Theory. *Phys. Rev. Lett.* **2010**, *105*, 146404.

(20) Kim, H. T.; Chae, B. G.; Youn, D. H.; Maeng, S. L.; Kim, G.; Kang, K. Y.; Lim, Y. S. Mechanism and observation of Mott transition in VO$_2$-based two- and three-terminal devices. *New J. Phys.* **2004**, *6*, 52.

(21) Cao, J.; Fan, W.; Chen, K.; Tamura, N.; Kunz, M.; Eyert, V.; Wu, J. Constant Threshold Resistivity in the Metal-Insulator Transition of VO$_2$. *Phys. Rev. B* **2010**, *82*, 241101.